

CALCULATION OF BNCT DOSIMETRY FOR BRAIN CANCER BASED ON KARTINI RESEARCH REACTOR USING THE PHITS CODE

Suhendra Gunawan Ntoy¹, Yohannes Sardjono²

¹Department of Physics, Faculty of Science and Mathematics,
Satya Wacana Christian University, Salatiga, 50711

²Particle Physics Division, Centre for Science and Accelerator Technology-National Nuclear Energy Agency,

Jl. Babarsari Kotak Pos Ykbb 6101, Sleman - Yogyakarta, 55281

Diterima editor: 2 September 2017

Diperbaiki: 16 Oktober 2017

Disetujui untuk publikasi: 17 Oktober 2017

ABSTRACT

CALCULATION OF BNCT DOSIMETRY FOR BRAIN CANCER BASED ON KARTINI RESEARCH REACTOR USING PHITS CODE. Cancer is a dangerous disease caused by the growth of a mass of cells that are unnatural and uncontrollable. Glioblastoma, also called as glioblastoma multiforme (GBM), is one of dangerous brain cancer. The dismal prognosis associated with glioblastoma is attributable not only to its aggressive and infiltrative behavior, but also to its location typically deep in the parenchyma of the brain. In resolving this challenge, the BNCT method can be a solution. This study aims to calculate BNCT dosimetry in different of cancer positions and irradiation geometries using PHITS code. The results show that the deeper the cancers target at brain the slower the total absorbed dose rate of cancer target. It takes a longer treatment time. Based on the treatment time and total absorbed dose rate of cancer target, the TOP irradiation geometry is an appropriate choice in treating the cancer target in this case. To achieve the histopathological cure of GBM at the primary site, the absorbed dose of brain was calculated to be 1.07 Gy and 1.64 Gy for the LLAT and PA irradiation geometry, respectively. While, for cancer position of 3 cm, 5 cm, 7.15 cm, 9 cm, and 11 cm, the absorbed dose of brain is 0.25 Gy, 0.48 Gy, 0.85 Gy, 1.33 Gy, and 2.01 Gy, respectively. In addition to the stochastic effect, it was found also deterministic effects that may be produced such as cataracts.

Keywords: BNCT dosimetry; GBM; brain cancer cases; PHITS; MIRD phantom

ABSTRAK

PERHITUNGAN DOSIMETRI BNCT PADA KANKER OTAK BERBASIS REAKTOR RISET KARTINI MENGGUNAKAN PROGRAM PHITS. Kanker merupakan salah satu penyakit berbahaya yang diakibatkan oleh tumbuhnya sekumpulan massa sel-sel yang tidak wajar dan tidak terkendali. Salah satu penyakit kanker otak yang berbahaya adalah Glioblastoma atau yang biasa disebut Glioblastoma Multiforme (GBM). Prognosis suram terkait dengan GBM tidak hanya untuk perilaku agresif dan infiltrasi, tetapi juga terhadap lokasi yang jauh di dalam parenkim otak. Untuk menjawab hal tersebut, Boron Neutron Capture Therapy (BNCT) dapat menjadi solusi. Penelitian ini bertujuan untuk menghitung dosimetri BNCT dalam berbagai posisi kerdan geometri penyinaran dengan menggunakan program PHITS. Hasil perhitungan menunjukkan bahwa semakin dalam target kanker di otak maka semakin kecil total laju dosis serap dari target kanker. Semakin dalam target kanker di otak dibutuhkan waktu pengobatan yang semakin lama. Berdasarkan waktu pengobatan dan laju dosis serap dari target kanker, bidang penyinaran TOP merupakan pilihan yang tepat dalam mengobati target kanker dalam kasus ini. Untuk mencapai penyembuhan GBM secara histopatologis di lokasi utama, dosis serap dari otak dihitung berturut-turut sebesar 1,07 Gy dan 1,64 Gy untuk bidang penyinaran LLAT dan PA. Sedangkan, untuk posisi kanker 3 cm, 5 cm, 7,15 cm, 9 cm, dan 11 cm, berturut-turut dosis serap dari otak adalah 0,25 Gy, 0,48 Gy, 0,85 Gy, 1,33 Gy, and 2,01 Gy. Selain adanya efek stokastik, ditemukan juga efek deterministik yang mungkin dihasilkan seperti katarak.

Kata kunci: Dosimetri BNCT, GBM, kanker otak, geometri penyinaran, posisi kanker, ORNL MIRD phantom.

INTRODUCTION

Cancer is a dangerous disease caused by the growth of a mass of cells that is unnatural and uncontrollable. According to the World Health Organization (WHO), approximately 8.2 million people die annually from cancer or an estimated 13% of all deaths worldwide [1]. In Indonesia, the GLOBOCAN estimated in 2012, for all ages and both sexes, the numbers of incidence and mortality of brain cancer reached 3402 and 4902 [2], respectively. According to that, Indonesia occupied the first rank in the Southeastern Asia. Glioblastoma, also called as glioblastoma multiforme (GBM), is one of dangerous brain cancer. GBM is a group of gliomas grade IV according to the WHO classification based on the increasing degree of anaplasia and aggressiveness [3]. Most studies reported that the survival of patients with GBM is quite short as compared with anaplastic astrocytoma and low-grade gliomas [4]. The dismal prognosis associated with glioblastoma is attributable not only to its aggressive and infiltrative behavior, but also to its location typically deep in the parenchyma of the brain [5]. Location GBM generally located in supratentorial areas such as frontal, temporal, parietal and occipital lobes [6,7]. The median overall survival of GBM patients with a deep location was 10 months and 24 months for GBM patients with superficial location [8]. It has been treated with various methods such as radiotherapy, chemotherapy, and surgery. However, the prognosis of GBM patients remain poor, median overall survival (OS) reached 11 months, and the 1-and 2 years OS rates were 45.9% and 7.7%, respectively. Therefore, the need for more effective novel treatments for this disease is urgently needed [9]. In resolving this challenge, Boron Neutron Capture Therapy (BNCT) can be a solution. Several countries have conducted research on BNCT as one of the GBM therapy types such as Japan, Finland, Taiwan, Germany, United States, Sweden, and Czech Republic [10]. It was found in the experience of BNCT clinical trials in Japan that for newly diagnosed GBM cases, median overall survival (OS) reached 25.7 months, and the 1- and 2-year OS rates were 85.7 % and 45.5 %, respectively [11]. Therefore, treatment for GBM patients with BNCT showed promising survival benefits. BNCT is a cancer treatment method designed to be selective in destroying cancer cells and saving healthy tissue cells [12]. This method is based on the irradiation of neutrons to cancer cells containing ^{10}B compound [13]. It causes fission reaction of ^7Li nuclei and alpha particles, where the linear energy transfers (LETs) value are $163 \text{ keV}/\mu\text{m}$ and $210 \text{ keV}/\mu\text{m}$, respectively [14]. Both of these particles have a high-LET as well as a short range of about one cell diameter resulting in a lethal dose only on cancer cells or tumors [15]. It is known as a boron dose, which is the main dose delivered to tumor cells or cancer. In addition to the boron dose, other major dose components such as nitrogen doses, gamma doses, and neutron doses are considered in the calculation of BNCT dosimetry [16].

BNCT-related research based on the Monte Carlo simulation has been done in recent years for brain cancer cases. In 2012, Rasouli and Masoudi used Beam Shaping Assembly (BSA) optimization design results to show that the weighted dose rate of the tumor target for a depth of 5.2 cm is 0.0372 Gy(w)/s [17]. In 2013, Herrera et al., showed that the minimum weighted dose rate delivered to the clinical target volume (CTV) was higher than 0.025 Gy(w)/s for the brain tumor (GBM) [18]. In 2014, Capoulat et al., investigated the reaction produced by $^9\text{Be(d, n)}^{10}\text{B}$ as a neutron source for BNCT. It was found that the maximum weighted dose rate of brain tumor for a depth of 4.8 cm was 0.0412 Gy(w)/s [19]. While in 2015, Brandão and Campos showed that the weighted dose rate of brain tumors was 0.0167 Gy(w)/s . It was obtained by combining ^{252}Cf brachytherapy and BNCT [20]. In 2016, Hang et al., designed BSA to provide high epithermal neutron flux based on the D-T neutron generator. It was found that the weighted dose rate of brain tumors at a depth of 6.75 cm was 0.022 Gy(w)/s [21]. In 2017, Hsieh et al., used BSA design based on a DD neutron generator to show that the weighted dose rate of brain tumors at a depth of 3 cm is 0.0196 Gy(w)/s [22]. This study aims to calculate BNCT dosimetry in different of cancer positions and irradiation geometries using the PHITS code. The PHITS code has been used for research related to BNCT [23, 24]. It can be used to evaluate the absorbed dose to each organ within the reference phantoms [25].

MATERIAL AND METHODS

Beam source

The beam source was obtained from the design of collimator in the radial piercing beam port of Kartini Reactor for BNCT [26]. It was operated at 100 kW. The beam source is made in the form of a circle with a radius of 1 cm. It consists of four source components, namely thermal neutron, epithermal neutron, fast neutron, and primary gamma-ray. The distance between the beam source and the phantom surface was set as 10 cm. Table 1 lists the source strength of each of the four components of the beam source for Kartini Reactor operated at 100 kW.

Table 1. Source strengths of the different components of the Kartini Reactor beam source.

Source particle	Energy range (MeV)	Beam aperture (radius of 1 cm)	
		Total source strength(s^{-1})	Average surface source strength ($cm^{-2} s^{-1}$)
Thermal neutron	0 ~ 5.00E-07	4.1409E+08	1.3181E+08
Epithermal neutron	5.00E-07 ~ 1.00E-02	3.0527E+08	9.7170E+07
Fast neutron	1.00E-02 ~ 1.80E+01	3.0184E+08	9.6080E+07
Total neutron	0 ~ 1.80 E+01	1.0212E+09	3.2506E+08
Primary gamma	0 ~ 1.80E+01	3.0355E+08	9.6622E+07

Patient model

In this study, GBM patient was defined as ORNL MIRD phantom [27] that was simulated in the PHITS code. The ORNL MIRD phantom has been used for BNCT-related research [28,29]. It was created by researchers at Hanyang University in Korea. The ORNL MIRD phantom is ready for use for BNCT dosimetry calculations and it is available at the Los Alamos National Laboratory database [30] and the Computational Medical Physics Working Group [31]. Three types of material compositions, namely, soft tissue, lung, and bone were used in the phantom. Fig. 1 shows the outline of the phantom without skin made with the PHITS code in three dimensions. Cancer target was assumed as the clinical target volume (CTV). It was defined as a sphere with radius of 1.5 cm. According to the data of 22 recurrent glioma patients were treated with BNCT in Finland, the ^{10}B concentration in blood in lies the range from 11 to 22 ppm, from 19 to 46 ppm in brain, and from 44 to 93 ppm in tumor under BPA-f infusion of 290-450 mg/kg during 2 hours [32]. Therefore, the ^{10}B concentration in the cancer target was reasonably taken as 60 and 20 ppm for the normal organs assuming that the ^{10}B concentrations in normal tissue and in blood are the same.

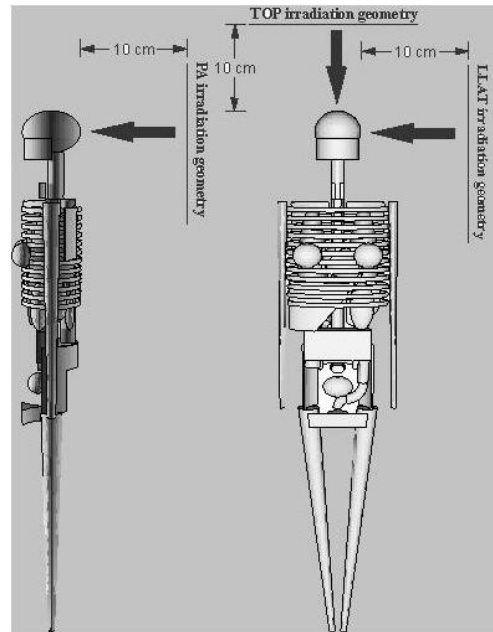


Figure 1. Outline and irradiation geometries of the ORNL MIRD phantom.

Calculation of BNCT dosimetry

The Monte Carlo code PHITS version 2.81[33] was applied to calculate BNCT dosimetry for clinical cases. The clinical cases that were selected to cover the study of brain cancer (GBM) are presented. This set of cases included superficial and deep cancer. In addition, the selection of appropriate irradiation geometry for the treatment of brain cancer was also involved. Therefore, the simulation in this study was conducted in two stages. In the first stage, it was performed to investigate the effect of different cancer positions toward the total absorbed dose rates of cancer target and some representative organs. Note that in the first stage, the TOP irradiation geometry was made constant. In the second stage, the simulation was performed to investigate the effect of different irradiation geometries toward the total absorbed dose rates of cancer target and some representative organs. Note that in the second stage, the cancer position of 7.15 cm was made constant. The cancer positions and irradiation geometry is shown in Table 2.

Table 2. Different of cancer positions and irradiation geometries.

Cancer position ^a (cm)	Irradiation geometry
3	TOP ^b
5	AP
7.15 ^c	LLAT
8	-
11	-

^aThe cancer position is the depth of cancer in the brain. It is defined as the distance between the skin and the center of mass of the tumor.

^bThe irradiation geometry is made constant in the first stage.

^cThe cancer position is made constant in the second stage. It defines the center of mass of the tumor.

The absorbed dose rate due to the neutron, gamma, $^{14}\text{N} (n, p)^{14}\text{C}$ reaction and $^{10}\text{B} (n, \alpha)^7\text{Li}$ reaction were determined separately. The absorbed dose due to $^{14}\text{N} (n, p)^{14}\text{C}$ and $^{10}\text{B} (n, \alpha)^7\text{Li}$ reaction were determined using the [T-DEPOSIT] tally. It is used to calculate energy loss of charged particles and nuclei. While, for the absorbed neutron and gamma dose, they were determined using the [T-

TRACK] tally and [MULTIPLIER] section considering kerma coefficients in the Dosimetry System 2002 (DS02) [34]. Note that the gamma dose is the sum of the secondary gamma dose which is generated of the $^1\text{H}(\text{n}, \gamma)^2\text{H}$ reaction and the primary gamma dose which is generated from primary gamma-ray sources.

Table 3. Relative- and compound biological effectiveness of different dose components for use in the calculation of BNCT dosimetry.

Dose component	RBE/CBE
Boron dose (D_B)	CBE=3.8:1.3 for cancer:normal organ
Nitrogen dose (D_N)	RBE= 3.2
Gamma dose (D_γ)	RBE= 1
Neutron dose(D_{nf})	RBE= 3.2

In term of BNCT, the weighted dose or commonly known as the total biologically weighted dose, is defined as [35]:

$$D_W = \text{CBE} \times D_B + \text{RBE} \times D_{nf} + \text{RBE} \times D_N + \text{RBE} \times D_\gamma \quad (1)$$

Where D_{nf} , D_γ , D_B dan D_N are the absorbed dose due to neutron, gamma, $^{10}\text{B}(\text{n}, \alpha)^7\text{Li}$ reaction, and $^{14}\text{N}(\text{n}, \text{p})^{14}\text{C}$ reaction, respectively. The values of Relative Biological Effectiveness (RBE) and Compound Biological Effect (CBE) are shown in Table 3 [36,37,18]. RBE is comparison of absorbed doses of radiation reference sources with test radiation that produce the same biological effect, whereas CBE is a factor of the biological effect used on boron carrier compound [38,39]. To illustrate the difference of the absorbed and weighted doses, the letter W in parenthesis is added to the symbol Gy writing one space between the symbol and the additional specification for the weighted dose (Gy (w) [40].

RESULTS AND DISCUSSION

The results of BNCT dosimetry calculations obtained in the first and second stages are shown in Table 4. In the first stage, Table 4 lists the total absorbed dose rates of cancer target and some representative organs for different cancer positions. Note that in the first stage, the TOP irradiation geometry is made constant. In the second stage, Table 4 also lists the total absorbed dose rates of cancer target and some representative organs for different irradiation geometry. Note that in the second stage, the cancer position of 7.15 cm is constant. In addition, the total weighted dose rates of cancer targets and some representative organs are included in Table 4. As shown in Table 4, the total weighted dose rate is greater than the total absorbed rate by a factor of 1.42-3.

Table 4. The total absorbed and weighted dose of cancer target and some representative organ

Cancer Position ^a (cm)	3	5	7.15 ^b	9	
Total absorbed dose (Gy)	Cancer	2.87E-03	1.73E-03	1.08E-03 (9.12E-04) ^c	(6.34E-04) ^d 7.54E-04
	Brain	4.84E-05	5.43 E-05	5.78E-05 (5.93E-05)	(6.02E-05) 5.95E-05
	Cranium	3.29E-05	3.30E-05	3.31E-05 (3.33E-05)	(3.28E-05) 3.31E-05
	Head and Neck Skin	1.41E-05	1.41E-05	1.41E-05 (1.46E-05)	(1.43E-05) 1.41E-05
	Thyroid	2.02E-06	2.05E-06	1.97E-06 (5.24E-06)	(3.89E-06) 2.03E-06
	Weighted dose rate (Gy)	Cancer	8.62E-03	4.96E-03	2.98E-03 (2.44E-03) ^c
Brain		1.18E-04	1.35E-04	1.45E-04 (1.45E-04)	(1.55E-04) 1.50E-04
Cranium		7.99E-05	8.02E-05	8.03E-05 (8.06E-05)	(8.05E-05) 8.02E-05
Head and Neck Skin		3.59E-05	3.59E-05	3.59E-05 (3.68E-05)	(3.66E-05) 3.59E-05
Thyroid		4.02E-06	4.10E-06	3.90E-06 (7.43E-06)	(3.78E-06) 4.07E-06

^aThe cancer position is the depth of cancer in the brain. It is defined as the distance between the skin and the center of mass of the tumor, ^bThe center of mass of the tumor, ^cLLAT irradiation geometry, ^dPA irradiation geometry

As shown in Table 4, for the first stage, the total absorbed dose rate of target cancer is significantly different at each cancer position. In other words, the deeper the cancer target at brain means the slower the total absorbed dose rate of cancer target. Table 4 also shows that the total absorbed dose rate of some representative organs such as cranium, head and neck skin, and thyroid are not significantly different in each cancer position. Meanwhile, the total absorbed dose rate of brain is significantly different in each cancer position. Seen in Table 4, the total absorbed dose rate of brain was increased in each cancer position. As expected, the total absorbed dose rate of target cancer is greater than the total absorbed dose rate of some representative organs for different cancer positions. For the second stage, the total absorbed dose rate of cancer target is significantly different in the irradiation geometry. The total absorbed dose rate of target cancer for the TOP irradiation geometry is greater than the total absorbed dose rate of target cancer for the LLAT and PA irradiation geometry. Regarding the average absorbed dose rate of brain and skin (skin of head and neck) as shown in Table 4, the TOP irradiation geometry is smaller than the LLAT and PA irradiation geometry. For the total absorbed dose rate of cranium, the LLAT irradiation geometry is greater than the TOP and PA irradiation geometry. For the total absorbed dose rate of thyroid, the TOP irradiation geometry is greater than the LLAT and PA irradiation geometry. However, the TOP irradiation geometry is an appropriate choice in treating the cancer target in this case. To achieve the histopathological cure of GBM at the primary site, the optimal minimal dose to the CTV was 44 Gy(w) [41]. Based on it and from the data in Table 4, the treatment time has been calculated for the first and second stages. These results are presented in Table 5.

Table 5. The treatment time for different of cancer positions and irradiation geometries

Cancer position ^a (cm)	Treatment time (hour)
3	1.42
5	2.46
7.15 ^b	4.11 (5.01) ^c (7.59) ^d
9	6.22
11	9.19

^aThe cancer position is the depth of cancer in the brain. It is defined as the distance between the skin and the center of mass of the tumor. ^bThe center of mass of the tumor ^cLLAT irradiation geometry ^dPA irradiation geometry

In the first stage, for cancer position of 3 cm, 5 cm, 7.15 cm, 9 cm, and 11 cm, the treatment time are 1.42 hours, 2.46 hours, 4.11 hours, 6.22 hours, and 9.19 hours, respectively. In the second stage, the treatment time is 5.01 hours and 1.64 hours for the LLAT and PA irradiation geometry, respectively. As shown in Table 5, the cancer target is getting deeper, thus requires a longer treatment time. Table 5 also shows that treatment time for the TOP irradiation geometry is faster than treatment time for the LLAT and PA irradiation geometry. From the data in Table 4 and the treatment time shown in Table 5, the absorbed doses of some representative organ has been calculated. These results are presented in Table 6. In addition, the total weighted dose of some representative organ is included in Table 6. As shown in Table 6, in the first stage, for cancer position of 3 cm, 5 cm, 7.15 cm, 9 cm, and 11 cm, the absorbed dose of brain is 0.25 Gy, 0.48 Gy, 0.85 Gy, 1.33 Gy, and 2.01 Gy, respectively. In the second stage, the absorbed doses of brain are 1.07 Gy and 1.64 Gy for the LLAT and PA irradiation geometry, respectively.

Table 6. The total absorbed and weighted dose of cancer target and some representative organ

Cancer Position ^a (cm)		3	5	7.15 ^b		9	11	
Total absorbed dose (Gy)	Brain	0.25	0.48	0.85	(1.07) ^c	(1.64) ^d	1.33	2.01
	Cranium	0.17	0.29	0.49	0.60	(0.90)	0.74	1.09
	Head and Neck Skin	0.07	0.13	0.21	0.26	(0.39)	0.32	0.47
	Thyroid	0.01	0.02	0.03	0.01	(0.01)	0.05	0.07
Weighted dose rate (Gy)	Brain	0.60	1.20	2.15	2.70	(4.23)	3.37	5.09
	Cranium	0.41	0.71	1.19	1.45	(2.20)	1.79	2.65
	Head and Neck Skin	0.18	0.32	0.53	0.66	(1.00)	0.80	1.19
	Thyroid	0.02	0.04	0.06	0.01	(0.02)	0.09	0.14

^aThe cancer position is the depth of cancer in the brain. It is defined as the distance between the skin and the center of mass of the tumor, ^bThe center of mass of the tumor, ^cLLAT irradiation geometry, ^dPA irradiation geometry

In addition to the stochastic effect related to the calculated absorbed dose, it was also found the deterministic effects that cannot be ignored in Table 6. According to the International Commission on Radiological Protection (ICRP), Assessment of the lens of the eye, skin, and extremity doses and methods of protection is necessary to improve occupational protection in interventional and nuclear medicine procedures [42]. Although the absorbed dose of the lens of the eye is not calculated on the ORNL MIRD phantom, it should be comparable to the absorbed dose of brain. Since the threshold absorbed dose of the lens of the eye is now considered to be 0.5 Gy[43], Cataracts may occur in GBM patients treated with therapy BNCT for cancer positions of 7.15 cm, 9 cm, and 11 cm.

CONCLUSION

BNCT dosimetry in brain cancer cases has been calculated using the PHITS code. The results show that the deeper the cancers target at brain means the slower the total absorbed dose rate of cancer target. It takes a longer treatment time. Based on the treatment time and total absorbed dose rate of cancer target, the TOP irradiation geometry is an appropriate choice in treating the cancer target in this case. To achieve the histopathological cure of GBM at the primary site, the absorbed dose of brain was calculated to be 1.07 Gy and 1.64 Gy for the LLAT and PA irradiation geometry, respectively. While, for cancer position of 3 cm, 5 cm, 7.15 cm, 9 cm, and 11 cm, the absorbed dose of brain is 0.25 Gy, 0.48 Gy, 0.85 Gy, 1.33 Gy, and 2.01 Gy, respectively. In addition to the stochastic effect, it was found also deterministic effects that may be produced such as cataracts.

ACKNOWLEDGMENT

The authors would like to express their thanks to those who took roles for the accomplishment of the project, especially for Dr. SuryasatriyaTrihandaruand JodelineMuningaras the Lecturer at Department of Physics of UKSW and Dr. Susilo Widodo as the Head of Centrefor AccaeleratorScience and Technology - National Nuclear Energy Agency (PSTA-BATAN) for the opportunity given to do this work.

REFERENCES

1. World Health Organization. Programmes and projects, Cancer, 2017. Available from: <http://www.who.int/cancer/en/>. Last accessed 08 January 2017.
2. As Ferlay J, Soerjomataram I, Ervik M, Dikshit R, Eser S, Mathers C et al. GLOBOCAN 2012 v1.0, Cancer Incidence and Mortality Worldwide: IARC CancerBase No. 11 [website]. Lyon, France: International Agency for Research on Cancer; 2013 (http://globocan.iarc.fr/old/bar_site.as, accessed 9 January 2017).
3. A. Omuro and L. M. DeAngelis, "Glioblastoma and Other Malignant Gliomas: A Clinical Review," *JAMA*, vol. 310, no. 17, pp. 1842–1850, Nov. 2013.
4. M. Penas-Prado, T. S. Armstrong, and M. R. Gilbert, "Chapter 32 - Glioblastoma," in *Handbook of Clinical Neurology*, 3rd series., vol. 105, W. G. and R. Soffietti, Ed. Elsevier, 2012, pp. 485–506.
5. R. D. Alkins, P. M. Brodersen, R. N. S. Sodhi, and K. Hynynen, "Enhancing drug delivery for boron neutron capture therapy of brain tumors with focused ultrasound," *Neuro-Oncology*, vol. 15, no. 9, pp. 1225–1235, May 2013.
6. J. P. Thakkar et al., "Epidemiologic and Molecular Prognostic Review of Glioblastoma," *Cancer Epidemiology and Prevention Biomarkers*, vol. 23, no. 10, pp. 1985–1996, Oct. 2014.
7. C. C. Koet et al., "Differentiation between Glioblastoma Multiforme and Primary Cerebral Lymphoma: Additional Benefits of Quantitative Diffusion-Weighted MR Imaging," *PLOS ONE*, vol. 11, no. 9, pp. 1–15, Sep. 2016.
8. K. K. Das et al., "Pediatric glioblastoma: clinico-radiological profile and factors affecting the outcome," *Child's Nervous System*, vol. 28, no. 12, pp. 2055–2062, Dec. 2012.
9. N. Ahmadloo et al., "Treatment outcome and prognostic factors of adult glioblastoma multiforme," *Journal of the Egyptian National Cancer Institute*, vol. 25, no. 1, pp. 21–30, Mar. 2013.
10. R. F. Barth et al., "Current status of boron neutron capture therapy of high grade gliomas and recurrent head and neck cancer," *Radiation Oncology*, vol. 7, no. 1, pp. 146–166, Jan. 2012.
11. K. Nakai, T. Yamamoto, H. Kumada, and A. Matsumura, "Boron Neutron Capture Therapy for Glioblastoma: A Phase-I/II Clinical Trial at JRR-4," *European Association of Neuro Oncology Magazine*, vol. 4, no. 3, pp. 116–123, Jun. 2014.
12. R. Ahangari and H. Afarideh, "Therapeutic gain prediction for evaluation and optimization of neutron spectra in BNCT," *Annals of Nuclear Energy*, vol. 49, pp. 212–217, Nov. 2012.
13. Y. Kasesaz, H. Khalafi, and F. Rahmani, "Design of an epithermal neutron beam for BNCT in thermal column of Tehran research reactor," *Annals of Nuclear Energy*, vol. 68, pp. 234–238, Jun. 2014.
14. N. Kondo et al., "Detection of γ H2AX foci in mouse normal brain and brain tumor after boron neutron capture therapy," *Reports of Practical Oncology & Radiotherapy*, vol. 21, no. 2, pp. 108–112, Mar. 2016.
15. Y. Kasesaz et al., "A feasibility study of the Tehran research reactor as a neutron source for BNCT," *Applied Radiation and Isotopes*, vol. 90, pp. 132–137, Aug. 2014.
16. M. Ziegner et al., "Confirmation of a realistic reactor model for BNCT dosimetry at the TRIGA Mainz," *Med. Phys.*, vol. 41, no. 11, p. 111706, Nov. 2014.
17. F. S. Rasouli and S. F. Masoudi, "Simulation of the BNCT of Brain Tumors Using MCNP Code: Beam Designing and Dose Evaluation," *Iranian Journal of Medical Physics*, vol. 9, no. 3, pp. 183–192, Sep. 2012.
18. M. S. Herrera, S. J. González, D. M. Minsky, and A. J. Kreiner, "Evaluation of performance of an accelerator-based BNCT facility for the treatment of different tumor targets," *Physica Medica: European Journal of Medical Physics*, vol. 29, no. 5, pp. 436–446, Sep. 2013.

19. M. e. Capoulat, M. s. Herrera, D. m. Minsky, S. j. González, and A. j. Kreiner, “ $^9\text{Be}(\text{d}, \text{n})^{10}\text{B}$ -based neutron sources for BNCT,” *Applied Radiation & Isotopes*, vol. 88, pp. 190–194, Jun. 2014.
20. S. F. Brandão and T. P. R. Campos, “Intracavitary moderator balloon combined with ^{252}Cf brachytherapy and boron neutron capture therapy, improving dosimetry in brain tumour and infiltrations,” *Br. J. Radiol.*, vol. 88, no. 1051, pp. 1–11, Jul. 2015.
21. S. Hang *et al.*, “Monte Carlo study of the beam shaping assembly optimization for providing high epithermal neutron flux for BNCT based on D–T neutron generator,” *Journal of Radioanalytical and Nuclear Chemistry*, vol. 310, no. 3, pp. 1289–1298, Dec. 2016.
22. M. Hsieh, Y. Liu, F. Mostafaei, J. M. Poulson, and L. H. Nie, “A feasibility study of a deuterium–deuterium neutron generator-based boron neutron capture therapy system for treatment of brain tumors,” *Med. Phys.*, vol. 44, no. 2, pp. 637–643, Feb. 2017.
23. K. Takada *et al.*, “Evaluation of the radiation dose for whole body in boron neutron capture therapy,” *Prog. Nucl. Sci. Technol.*, vol. 4, pp. 820–823, 2014.
24. H. Kumada, K. Takada, K. Yamanashi, T. Sakae, A. Matsumura, and H. Sakurai, “Verification of nuclear data for the Tsukuba plan, a newly developed treatment planning system for boron neutron capture therapy,” *Appl. Radiat. Isot.*, vol. 106, pp. 111–115, Dec. 2015.
25. C. H. Clement *et al.*, “Conversion Coefficients for Radiological Protection Quantities for External Radiation Exposures,” *Ann. ICRP*, vol. 40, no. 2–5, pp. 1–257, Apr. 2010.
26. M. limaMuslih, Y. Sardjono, and A. Widiarto, “Perancangan Kolimator Di Beam Port Tembus Reaktor Kartini Untuk Boron Neutron Capture Therapy,” *Pus. Sains Dan Teknologi Akselerator - BATAN*, pp. 163–178, Jun. 2014.
27. Eckerman KF, Cristy M, Ryman JC. The ORNL mathematical phantom series. Oak Ridge, TN: Oak Ridge National Laboratory. 1996 Dec.
28. D. Krstic, V. M. Markovic, Z. Jovanovic, B. Milenkovic, D. Nikezic, and J. Atanackovic, “Monte Carlo calculations of lung dose in ORNL phantom for boron neutron capture therapy,” *Radiat. Prot. Dosimetry*, vol. 161, no. 1–4, pp. 269–273, Oct. 2014.
29. J. N. Wang, C. K. Huang, W. C. Tsai, Y. H. Liu, and S. H. Jiang, “Effective dose evaluation for BNCT treatment in the epithermal neutron beam at THOR,” *Appl. Radiat. Isot.*, vol. 69, no. 12, pp. 1850–1853, Dec. 2011.
30. A. D. Lazarine, *Medical physics calculations with MCNP: a primer*. Texas A&M University, 2006. [Online]. Available: <http://oaktrust.library.tamu.edu/handle/1969.1/4297> [Accessed: 02-Juni2017].
31. R. Zhang and ArzuAlpan, “Computational Medical Physics Working Group.” [Online]. Available: <http://cmpwg.ans.org/members.html>. [Accessed: 29-May-2017].
32. H. Koivunoroet *al.*, “Biokinetic analysis of tissue boron (^{10}B) concentrations of glioma patients treated with BNCT in Finland,” *Applied Radiation and Isotopes*, vol. 106, pp. 189–194, Dec. 2015.
33. T. Sato *et al.*, *J. Nucl. Sci. Technol*, vol. 50, pp. 913–923, 2013.
34. Kerr, George D., Pace, Joseph V. III, & Egbert, Stephen D. Young, Robert W., & Kerr, George D. (Eds.). (2005). Survivor dosimetry Part a Fluence-to-kerma conversion coefficients (INISJP--102). Young, Robert W., & Kerr, George D. (Eds.). Japan
35. N. Ghal-Eh, H. Goudarzi, and F. Rahmani, “FLUKA simulation studies on in-phantom dosimetric parameters of a LINAC-based BNCT,” *Radiat. Phys. Chem.*, vol. 141, pp. 36–40, Dec. 2017.
36. Z. A. Ganjeh and S. F. Masoudi, “Neutron beam optimization based on a $^7\text{Li}(p, n)^7\text{Be}$ reaction for treatment of deep-seated brain tumors by BNCT,” *Chin. Phys. C*, vol. 38, no. 10, p. 108203, 2014.
37. F. Torabi, S. FarhadMasoudi, F. Rahmani, and F. Rasouli, “BSA optimization and dosimetric assessment for an electron linac based BNCT of deep-seated brain tumors,” *J. Radioanal. Nucl. Chem.*, vol. 300, no. 3, pp. 1167–1174, Jun. 2014.

38. L. Evangelista, G. Jori, D. Martini, and G. Sotti, "Boron neutron capture therapy and ^{18}F -labelled borophenylalanine positron emission tomography: A critical and clinical overview of the literature," *Appl. Radiat. Isot.*, vol. 74, pp. 91–101, Apr. 2013.
39. T. Watanabe, H. Tanaka, S. Fukutani, M. Suzuki, M. Hiraoka, and K. Ono, "L-phenylalanine preloading reduces the ^{10}B (n, α) ^7Li dose to the normal brain by inhibiting the uptake of boronophenylalanine in boron neutron capture therapy for brain tumours," *Cancer Lett.*, vol. 370, no. 1, pp. 27–32, Jan. 2016.
40. International Atomic Energy Agency, Vienna (Austria) (2001). *Current status of neutron capture therapy* (IAEA-TECDOC--1223). International Atomic Energy Agency (IAEA)
41. T. Kageji, Y. Mizobuchi, S. Nagahiro, Y. Nakagawa, and H. Kumada, "Correlation between radiation dose and histopathological findings in patients with glioblastoma treated with boron neutron capture therapy (BNCT)," *Applied Radiation and Isotopes*, vol. 88, pp. 20–22, Jun. 2014.
42. ICRP, 2017 ICRP Statement on "Areas of Research to Support the System of Radiological Protection", [Online]. Available: <http://www.icrp.org/docs/ICRP%20Research%20Priorities%202017.pdf> [Accessed: 8-August-2017].
43. ICRP, 2012 ICRP Statement on Tissue Reactions / Early and Late Effects of Radiation in Normal Tissues and Organs – Threshold Doses for Tissue Reactions in a Radiation Protection Context. ICRP Publication 118. Ann. ICRP 41(1/2).